KONSTAN
JURNAL FISIKA DAN PENDIDIKAN FISIKA
Volume 9, Number 1, June 2024
E-ISSN: 2460-9129 dan P-ISSN: 2460-9110
http://jurnalkonstan.ac.id/index.php/jurnal

STUDY OF MICROSTRUCTURE, MORPHOLOGY AND FUNCTIONAL GROUPS OF TITANIUM DIOXIDE (TIO_2) IMPREGNATED WITH COPPER (CU)

La Ode Asmin[1,*], La Isa[1]

[1]*Institut Agama Islam Negeri (IAIN) Kendari, Kendari, Indonesia*

*E-mail korespondensi: fisikakuanta@gmail.com

Article Info:

Sent:
December 20, 2023

Revision:
May 18, 2024

Accepted:
July 2, 2024

Keywords:
Microstructure, Morphology, Functional groups, Impregnation, Copper, TiO_2.

Abstract

This research aims to determine the differences in the microstructure, morphology, and functional groups of TiO_2 (P-25) after being impregnated with Cu. Cu-impregnated TiO_2 samples are synthesized using the impregnation method with TiO_2 (P-25) and copper sulfate as precursors. The microstructure and functional groups of TiO_2 (P-25) and Cu-TiO2 were investigated using X-ray diffraction (XRD), scanning electron microscope-energy dispersive x-ray (SEM-EDX), and Fourier transform infrared (FTIR) analysis. The lattice parameters (a, b, and c) of the TiO_2 sample were found to be a = b = 0.3778 nm, c = 0.9494 nm, and these values increased to a = b = 0.3779 nm, c = 0.9496 nm after the addition of Cu. The distance between the lattices of the TiO_2 sample was measured at 0.3505 nm and increased to 0.3509 nm after Cu addition. The average crystallite size of the TiO_2 sample was 33 nm, which increased to 43 nm after Cu impregnation. The strain value decreased from 2.76×10^(-3) to 1.82×10^(-3) after Cu addition. SEM results revealed that the morphology of the particles from the Cu-doped synthesis showed agglomeration. The success of Cu doping was confirmed by EDX mapping, which showed the presence of Ti, O, and Cu evenly distributed on the TiO_2 surface. The FTIR spectrum indicated that TiO_2 (P-25) and Cu-TiO_2 particles had absorption peaks at similar wave numbers. However, in the absorption area of 1000 cm^-1 to 1250 cm^-1, new absorption bands affiliated with Cu-O bonds appeared in the Cu-TiO_2 sample, resulting from TiO_2 vibrations after Cu addition.

© 2024 State Islamic University of Mataram

INTRODUCTION

Among semiconductor oxides, titanium dioxide (TiO_2) nanomaterials have been widely studied in the last two decades [1]. TiO_2 is interesting to research because of its unique properties and applications in various fields. Among the properties of TiO_2 are good optical transmittance, high refractive index, and stability. Due to its properties, TiO_2 nanomaterial is used in many applications, including paint, toothpaste, UV protection, photocatalysis, photovoltaic, electrochromic, and photochromic [2]. TiO_2 exists in three phases, namely anatase, brookite, and rutile [3].

In recent years, research related to TiO_2 doping with transition metals has been routinely carried out. Doping TiO_2 with metal can change the physical properties of TiO_2 [4]. In practice, TiO_2

can only respond to photons in the wavelength range of ultraviolet light, which accounts for only 5% of sunlight. So, it is important to expand the wavelength range to the visible light region, which covers 45% of the sun. An effective strategy to increase the visible light sensitivity of TiO_2 is doping with elements [5]. This will make TiO_2 work more efficiently as a photocatalyst. Several literatures have reported the synthesis and characterization process of TiO_2 powder doped with transition metals including iron (Fe)[6], nickel (Ni)[7], manganese (Mn)[8], magnesium (Mg) [9], dan copper (Cu). Among the doping elements, copper (Cu) is one of the dopants that can increase visible light absorption and photocatalytic efficiency [10]. Apart from that, copper (Cu) has an ionic radius that is not much different, namely Cu^{2+} (0.72 Å) is almost identical to Ti^{4+} (0.68 Å) [11]. In its application, the Cu atom is an antibacterial element [12]. So doping TiO2 with Cu can expand its application area.

Many methods have been used for the preparation of Cu-TiO2 including coprecipitation [4], liquid phase deposition techniques [13], impregnation [14], [15], and sol-gel [16]. Kaya and Türkten, [17] synthesized TiO2 doped with non-metals (C, N, Se), metals (Cu, Fe), and co-doping (N/S) using the wet impregnation method and obtained changes in optical properties. TiO_2 shifts its band gap energy from 3.2 eV to lower, namely 2.55-2.90 eV. Leong et al [18] also reported the use of different methods to synthesize Cu-TiO_2, namely sonochemical, impregnation, and physical mixing methods. The result is that the sample forms a rutile phase with high crystallinity, smaller particle size with a larger sample surface area. In addition, there is a decrease in the band gap energy in the sample, so it is active in the visible light wavelength range.

In this research, the synthesis of Cu-TiO_2 was carried out using the impregnation method, because it is fast and cheap. In addition, the impregnation method can control the configuration, crystallography, and morphology of the sample [19]. X-ray diffraction (XRD), scanning electron microscope-energy dispersive x-ray (SEM-EDX), and Fourier transform infrared (FTIR) were used to characterize the resulting samples. In addition, the lattice strain values were also investigated.

RESEARCH METHODS

Synthesis of Cu-TiO_2

Cu-TiO_2 nanoparticles were synthesized using the impregnation method with $CuSO_4.5H_2O$ precursor and Degusa TiO_2 (P-25) (Merck). A total of 0.21 grams of $CuSO_4.5H_2O$ was dissolved in 50 ml of distilled water and stirred for 30 minutes at room temperature (solution X) at a speed of 120 rpm. Next, 3 grams of TiO_2 were added to solution X. The mixed solution was then stirred for 120 minutes at a temperature of 90^0C with a speed of 500 rpm. Next, the sample was dried in an oven at 110^0C for 30 minutes and ground until smooth. The Cu-TiO_2 powder sample was calcined at 500^0C for 180 minutes.

Characterization

The Cu-TiO_2 sample was characterized for analysis of the structure and phases formed using X-ray diffraction (XRD) Merck PANalytical, Type: Cu metal target material. Crystal size, lattice spacing, lattice parameters, and cell volume were calculated using equations (1)-(4) respectively.

$$t = \frac{k\lambda}{\beta \cos\theta} \quad (1)$$

$$d = \frac{n\lambda}{2\sin\theta} \quad (2)$$

$$\frac{1}{d^2} = \frac{h^2+k^2}{a^2} + \frac{l^2}{c^2} \quad (3)$$

$$V = a^2c \quad (4)$$

where t is the crystal grain size, k is Scherrer's constant (0.9), λ is the X-ray wavelength (in Å), β is the half-peak width (in radians), and θ is the Bragg diffraction angle (in radians), d is the interplanar distance, a and c are lattice parameters, h, k, and l are miller index notation.

Analysis of surface morphology and elements using Scanning Electron Microscopy/Energy Dispersive X-Ray (SEM/EDX) spectroscopy (mapping) HITACHI SU-3500 brand, EDX detector HORIBA brand. Measurement conditions were carried out at room temperature (18-

25) ^{0}C with room humidity <65%. Functional group analysis using Fourier Transform Infrared (FTIR) spectroscopy Brand Shimadzu, Type: IRPrestige 21.

RESULT AND DISCUSSION

X-ray diffraction

Figure 1 shows the XRD patterns of TiO_2 (P-25) and Cu-doped TiO_2 nanoparticles classed at 500^{0}C for 3 hours. The sample shows peaks corresponding to the anatase phase with a tetragonal system affiliated to the miller indices (101), (103), (004), (112), (200), (105), (211), (204), (116).), (220), and (215) (JCPDS No. 21−1272). The XRD diffraction pattern of anatase has a maximum peak at an angle of $2\theta = 25.888^0$ for TiO_2 (P-25) and $2\theta = 25.361^0$ for Cu-TiO_2. Garg et al., 2017 also observed the anatase phase at the angle $2\theta = 25.3685^0$ which is affiliated with the Miller index (101) [20].

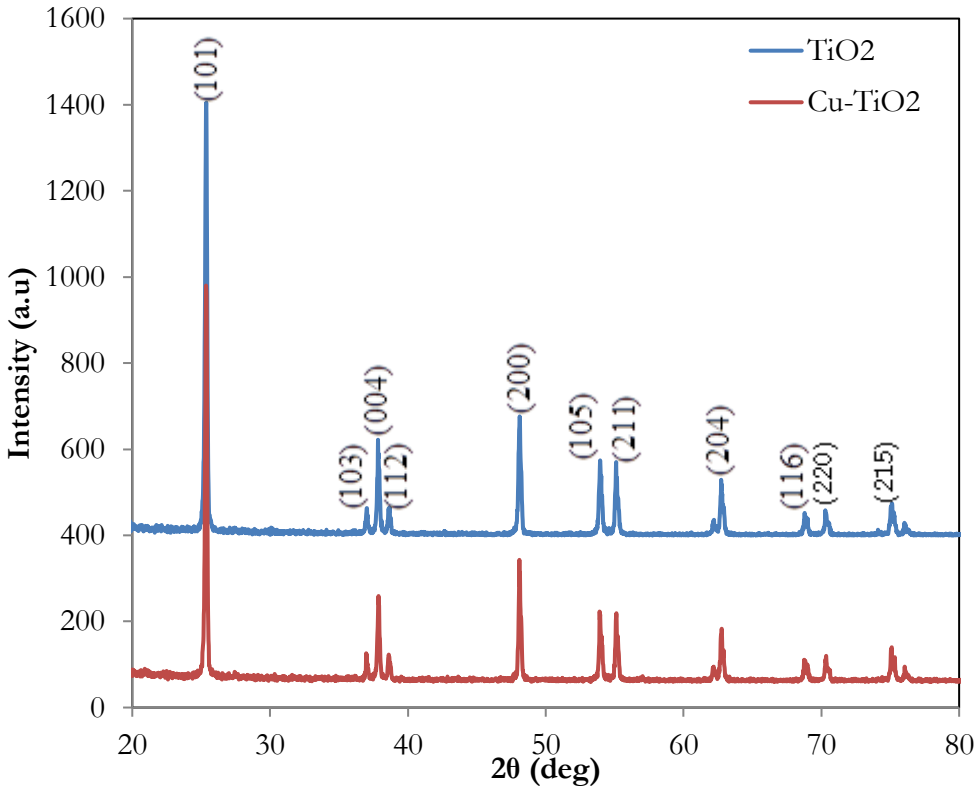

Gambar 1. XRD pattern of TiO_2 P-25 and Cu-TiO_2

The presence of a Cu peak was not observed, which indicates that Cu has been doped into the TiO_2 lattice. It also indicates that Cu is in amorphous or small crystalline form, which cannot be detected by XRD devices [21]–[23]. In addition, the absence of metal oxide diffraction peaks indicates good metal dispersion on the catalyst surface, in this case, TiO_2 [20], [24]. These results are supported by observations reported by Sahoo and Gupta, 2015 [25]. Another thing that causes the Cu metal diffraction peak to not be detected is the very low metal ion content [10].

Table 1. Cell volume and intensity of TiO_2 and Cu-TiO_2

Sample	Average FWHM	Volume (nm^3)	Intensity
TiO_2	0.291	0.1355	862.283
Cu-TiO_2	0.188	0.1356	893.706

Based on Table 1, it appears that the cell volume increases after adding Cu. The level of nanoparticle crystallinity can be identified by looking at the diffraction peak profile that appears and the phase composition that appears in the resulting sample. Compared to pure TiO_2 (P-25), the Cu-TiO_2 sample shows an increase in intensity which indicates that the quality of the

crystallites is getting better. In addition, the average FWHM obtained decreased from 0.291 for TiO_2 (P-25) to 0.188 for Cu-TiO_2, respectively. Based on the diffraction peaks that appear, the (101) peak on TiO2 and Cu-TiO_2 has a greater intensity than the other peaks. This indicates that the crystallite grains that appear have a preference for the (101) direction.

Microstructural and Morphological Analysis

Based on the X-ray diffraction pattern (Figure 1), estimates of the lattice parameters a and c, the crystallite size (t), the distance between planes (d_{hkl}), and strain (ε) can be obtained. Table 2 is the value of the lattice parameters a and c, calculated from the diffraction peak values (200) and (004), using equation (3) (with Miller indices for tetragonal systems).

Table 2. Lattice parameter values of TiO_2 and Cu-TiO_2

Sample	Lattice parameter	
	$a = b$ (nm)	c (nm)
TiO_2	0.3778	0.9494
Cu-TiO_2	0.3779	0.9496

Based on Table 2, it appears that the lattice parameters a and c of the TiO_2 sample experienced an insignificant increase after the addition of Cu. This is caused by the ion radius of Cu^{2+} (0.72 Å) being greater than Ti^{4+} (0.68 Å) [11]. This result is supported by observations made by Garg et al, 2017 and Jacoski, 2022, where TiO_2 doped with Cu experienced an increase [20][27].

Apart from knowing the crystal structure, from the results of characterization using XRD, the full width at half maximum (FWHM) value is also known. The smaller the FWHM value, the better the crystal quality, so the smaller the strain that occurs. A smaller FWHM value indicates that it is easier for adjacent atoms to adjust direction. The lattice strain value was obtained using the tangent formula (5) [28], the results of which are presented in Table 2.

$$\varepsilon = \frac{\beta}{4 \tan \theta} \tag{5}$$

Table 3. Peak position, FWHM, crystallite size and lattice strain of TiO_2 and Cu-TiO_2

TiO_2				**Cu-TiO_2**			
2-theta ($2\theta^0$)	d-spacing (nm)	Crystallite Size, t (nm)	Lattice Strain (ε)	2-theta ($2\theta^0$)	d-spacing (nm)	Crystallite Size, t (nm)	Lattice Strain (ε)
25.388	0.3505	39	0.00419	25.361	0.35092	47	0.00352
37.003	0.2427	53	0.00202	37.013	0.24268	52	0.00207
37.874	0.2374	29	0.00354	37.869	0.23739	43	0.00243
38.593	0.2331	47	0.00218	38.706	0.23245	45	0.00224
48.127	0.1889	11	0.00699	48.118	0.18895	37	0.00207
53.954	0.1698	17	0.00390	53.973	0.16975	31	0.00210
55.127	0.1665	17	0.00368	55.146	0.16642	32	0.00199
62.656	0.1482	31	0.00129	62.769	0.14791	31	0.00170
68.823	0.1363	20	0.00226	68.601	0.13669	49	0.00093
70.375	0.1337	34	0.00130	70.366	0.13369	29	0.00149
75.104	0.1264	57	0.00069	75.101	0.12639	57	0.00068
76.050	0.1250	36	0.00106	76.071	0.12502	62	0.00061

The peak position corresponding to the Miller index (101) experiences a small shift to a lower angle. This indicates that the crystal is distorted by the incorporation of Cu dopant because the ionic radius of Cu^{2+} is greater than Ti^{4+}. Cu substitution in Ti in the TiO_2 crystal lattice results in an increase in the interplanar distance. The distance between the lattices is almost the same, namely 0.3505 nm (TiO_2) and 0.3509 nm (Cu-TiO_2). This value is almost the same as the value

of the inter-lattice distance for the (101) diffraction peak given by JCPDS-21-1272 for anatase, namely 0.352 nm.

The average crystallite size of the samples was calculated from the full width at half maximum (FWHM) with the Debye-Scherer formula. and obtained 33 nm for pure TiO_2 (P-25). and 43 nm for Cu-TiO_2. These results indicate that the size of TiO_2 crystallites increases after the addition of Cu. This increase in crystallite size shows that Cu doping affects the growth of TiO_2 crystallites in the synthesis process. Based on the results of research conducted by [29] [30], the size of Cu-TiO2 crystallites slightly increased due to the presence of Cu2+ and CuO species. Different radii of Cu and Ti ions cause lattice distortion and strain fields thereby changing the size of Cu-TiO_2 crystallites [31]. When Cu ions replace Ti. The lattice parameters will increase and become larger resulting in the average size of the crystallites becoming larger. Replacement of Ti ions by Cu ions will affect the distribution of cations in the nanoparticles.

The average lattice strain values for TiO_2 (P-25) and Cu−TiO_2 were obtained as 2.76×10^{-3} and 1.82×10^{-3}, respectively. These results show that the strain decreased after adding Cu. Lattice strain measures the distribution of lattice constants that arise from crystal imperfections. Like lattice dislocations. as a result of changes in cation distribution. Crystal size and lattice strain influence peak broadening [32].

Figure 2(a) shows the SEM image of Cu-doped TiO_2 and 2(b-d) is the EDX mapping.

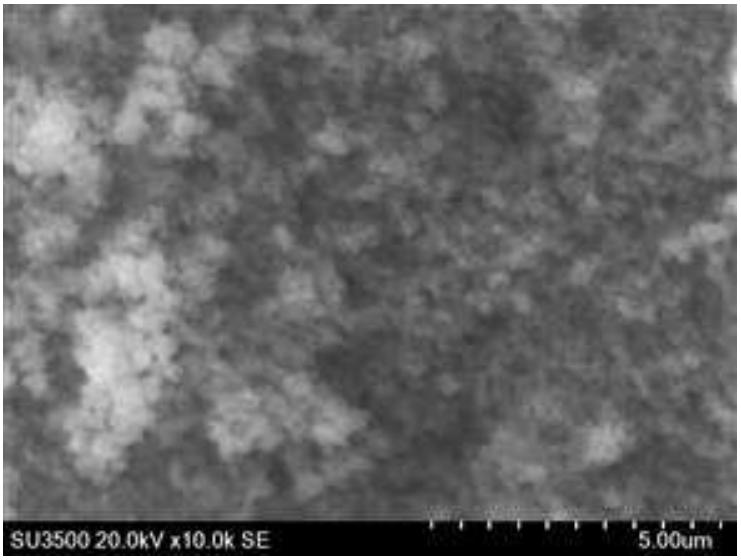

(a)

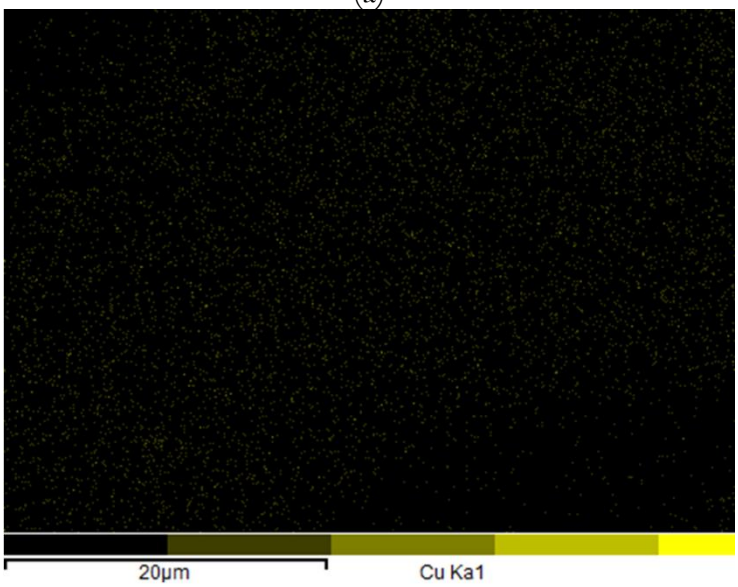

(b)

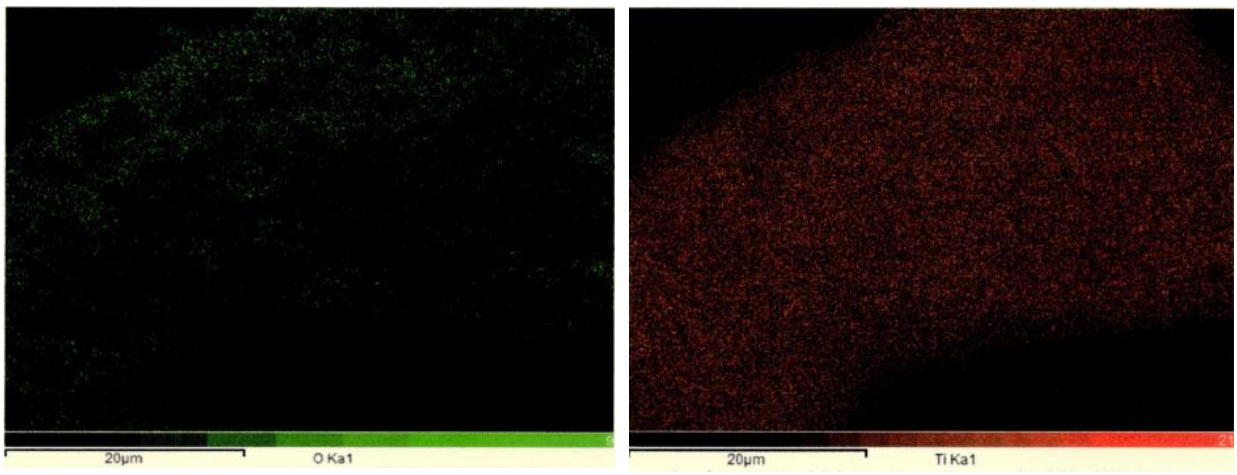

(c) (d)

Figure 2. (a) SEM image of the Cu-doped TiO_2 and (b-d) EDX mapping

SEM results show that the samples obtained tend to clump. Distribution of Cu elements on the TiO_2 surface. Analyzed by X-ray elemental mapping. as shown in Figure 2(b)-(d). From energy-dispersive X-ray spectroscopy (EDX) and elemental mapping patterns. We can see the presence of Ti, O, and Cu. The mapped elements are shown as coloured spots. The Cu element is evenly distributed on the TiO_2 surface. These results indicate that the synthesis method has succeeded in doping Cu onto the TiO_2 surface. This observation shows the formation of a Cu–TiO_2 composite material.

Functional Group Analysis

Fourier transform infrared (FTIR) spectroscopy shows the presence of TiO_2 (P-25) and Cu-TiO_2 functional groups. The FTIR transmission spectrum of TiO_2(P-25) and Cu-TiO_2 in the range 400 cm^{-1}-4000 cm^{-1} is shown in Figure 3. The peaks observed in TiO_2 (P-25) and Cu-TiO_2 show some of the same peaks. But there is also a new peak that appears when doped with Cu.

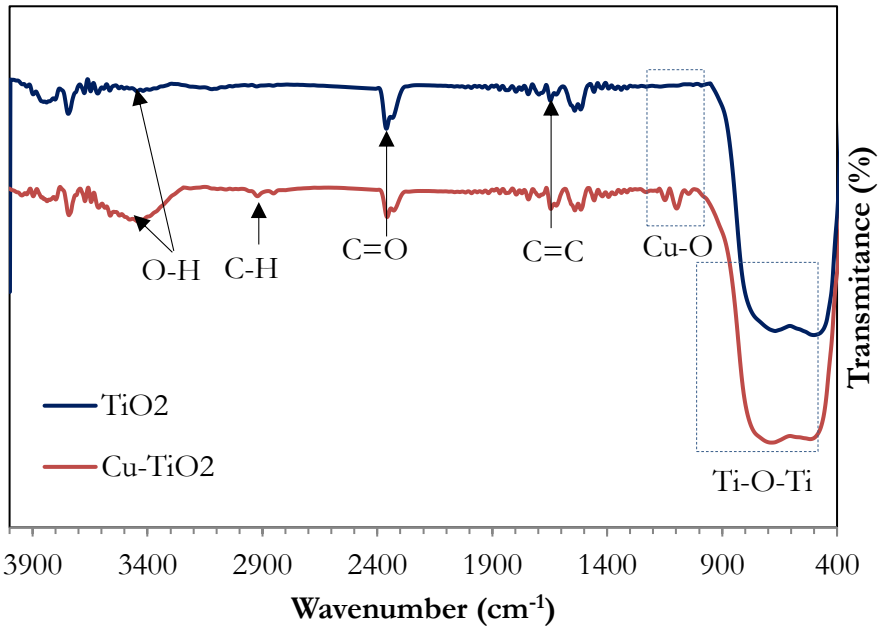

Figure 3. FTIR spectrum of TiO_2 and Cu-TiO_2 samples

In the absorption peak range of 500 cm^{-1} to 1000 cm^{-1}, it is related to the vibration absorption of the Ti-O-Ti bond. Based on Figure 3, the Ti-O-Ti structure appears in the absorption area of 501.49 cm^{-1} and 669.30 cm^{-1} for the TiO_2 anatase sample and 516.92 cm^{-1} and 686.66 cm^{-1} for Cu-TiO_2, which is the vibration characteristic of Ti-O. This result was also reported by Aritonang et al.. [33] who stated that the absorption area of 450-600 cm^{-1} was Ti-O

vibration. These results show that the absorption peak of TiO2 has shifted to a higher wavelength region after doping. The TiO_2 spectrum also shows absorption at the wave number 3444.72 cm^{-1} which is the -OH stretching absorption area of Ti-OH on the TiO_2 surface. This result is based on research conducted by Dong et al [34] stated that the wave number range of 3200-3500 cm-1 is the area of absorption of hydroxyl groups (-OH). Meanwhile, in the Cu-TiO_2 spectrum, it appears in the wave number absorption area of 3562.52 cm^{-1}. These results indicate a shift in the –OH absorption peak of TiO_2 after Cu was added to a higher wave number region. This shows that the shift in vibration absorption indicates that the Cu dopant has successfully entered the TiO_2 structure. At 1658.78 cm^{-1} is related to the -OH bending of Ti-OH on the TiO_2 surface [33]. However, the –OH absorption area obtained was at a wave number of 3446 cm^{-1}, slightly larger than the results of this study. Meanwhile, the Ti-OH absorption area was found to be smaller, namely at a wave number of 1635 cm^{-1}.

Besides that. Bond vibrations were also observed in the wave number range of 1000-1250 cm^{-1} after the addition of Cu. which was identified as a Cu-O bond resulting from TiO_2 lattice vibrations as a result of the presence of the Cu element [31]. The same results were also reported by [35]. The peak around 1622.13 cm^{-1} is C=C and 2357.01 cm^{-1} is the C=O absorption peak [31]. Here is a fundamental difference in the FTIR transmission spectrum for TiO_2 and Cu-TiO_2, namely in the wavelength range of 3300 cm^{-1} to 3800 cm^{-1}. Besides that. A new absorption area appears in the Cu-TiO_2 sample at the absorption peak from 2800 cm^{-1} to 3300 cm^{-1}. as also reported by Yan et al.. [36]. Namely in the 2850 cm^{-1} and 2920 cm^{-1} areas which are C-H stretching vibrations. This indicates that Cu doping on TiO_2 was successfully carried out using the impregnation method.

CONCLUSION

TiO_2 (P-25) samples and Cu-TiO_2 nanoparticles have been synthesized using the impregnation method. Microstructure, morphology, and the functional groups of TiO_2 (P-25) and Cu-TiO_2 nanoparticles have been studied based on data from characterization using XRD, SEM-EDX, and FTIR. Based on XRD results, the crystal structure shows the anatase phase. The lattice parameters (a, b, and c) of the TiO_2 sample were obtained $a = b = 0.3778$ nm, $c = 0.9494$ nm and increases after adding Cu, namely $a = b = 0.3779$ nm, $c = 0.9496$ nm. The cell volume and diffraction peak intensity of the TiO_2 sample increased after the addition of Cu. The distance between the lattices of the TiO_2 sample was found to be 0.3505 nm and increased after adding Cu to 0.3509 nm. The TiO_2 sample has an average crystallite size of 33 nm and increases after adding Cu to 43 nm (Cu-TiO_2). Meanwhile, the strain value decreased after adding Cu from 2.76×10^{-3} to 1.82×10^{-3}. Based on the SEM test results, the morphology of the particles resulting from the synthesis of agglomerated Cu doping was obtained. The success of Cu doping is demonstrated by the EDX mapping results. This indicates the presence of Ti, O, and Cu are evenly distributed on the TiO_2 surface. The FTIR spectrum shows that TiO_2 (P-25) and Cu-TiO_2 particles tend to have absorption peaks at the same wave number. However, in the absorption area of 1000 cm-1 to 1250 cm^{-1}, new absorption appears in the Cu-TiO_2 sample which is affiliated with Cu-O bonds as a result of TiO_2 vibrations after the addition of Cu.

REFERENCES

[1] L. Rohmawati *et al.*. "The characteristics of TiO2 anatase from tulungagung sand as an antibacterial material." *Nanosyst. Physics. Chem. Math.*. vol. 13. no. 6. pp. 640–648. 2022. doi: 10.17586/2220-8054-2022-13-6-640-648.

[2] S. T. Hayle. "Synthesis and Characterization of Titanium Oxide Nanomaterials Using Sol-Gel Method." *Am. J. Nanosci. Nanotechnol.*. vol. 2. no. 1. p. 1. 2014. doi: 10.11648/j.nano.20140201.11.

[3] R. Mutsak Ahmed and I. Hasan. "A review on properties and applications of TiO2and associated nanocomposite materials." *Mater. Today Proc.*. vol. 81. no. 2. pp. 1073–1078. 2021.

doi: 10.1016/j.matpr.2021.04.381.

[4] H. Sokoidanto. A. Taufik. and R. Saleh. "Structural and optical study of Cu-doped TiO2 nanoparticles synthesized by co-precipitation method." *J. Phys. Conf. Ser.*. vol. 1442. no. 1. pp. 0–6. 2020. doi: 10.1088/1742-6596/1442/1/012008.

[5] A. Khlyustova. N. Sirotkin. T. Kusova. A. Kraev. V. Titov. and A. Agafonov. "Doped TiO2: The effect of doping elements on photocatalytic activity." *Mater. Adv.*. vol. 1. no. 5. pp. 1193–1201. 2020. doi: 10.1039/d0ma00171f.

[6] T. Abza. A. Saka. J. L. Tesfaye. L. Gudata. N. Nagaprasad. and R. Krishnaraj. "Synthesis and Characterization of Iron Doped Titanium Dioxide (Fe: TiO2) Nanoprecipitate at Different pH Values for Applications of Self-Cleaning Materials." *Adv. Mater. Sci. Eng.*. vol. 2022. 2022. doi: 10.1155/2022/2748908.

[7] B. Surendra. B. M. Raju. K. N. S. Onesimus. G. L. Choudhary. P. F. Paul. and M. Vangalapati. "Synthesis and characterization of Ni doped TiO2 nanoparticles and its application for the degradation of malathion." *Mater. Today Proc.*. vol. 26. no. xxxx. pp. 1091–1095. 2019. doi: 10.1016/j.matpr.2020.02.216.

[8] M. Lešnik *et al.*. "Hydrothermal synthesis of mn-doped TiO2 with a strongly suppressed photocatalytic activity." *Mater. Tehnol.*. vol. 52. no. 4. pp. 411–416. 2018. doi: 10.17222/mit.2017.012.

[9] K. Athira. K. T. Merin. T. Raguram. and K. S. Rajni. "Synthesis and characterization of Mg doped TiO2nanoparticles for photocatalytic applications." *Mater. Today Proc.*. vol. 33. no. xxxx. pp. 2321–2327. 2020. doi: 10.1016/j.matpr.2020.04.580.

[10] C. Karunakaran. G. Abiramasundari. P. Gomathisankar. G. Manikandan. and V. Anandi. "Cu-doped TiO2 nanoparticles for photocatalytic disinfection of bacteria under visible light." *J. Colloid Interface Sci.*. vol. 352. no. 1. pp. 68–74. 2010. doi: 10.1016/j.jcis.2010.08.012.

[11] H. Liu and L. Gao. "Preparation and properties of nanocrystalline α-Fe 2O 3-sensitized TiO 2 nanosheets as a visible light photocatalyst." *J. Am. Ceram. Soc.*. vol. 89. no. 1. pp. 370–373. 2006. doi: 10.1111/j.1551-2916.2005.00686.x.

[12] K. Suzuki *et al.*. "Antibacterial properties of Cu-doped TiO2 prepared by chemical and heat treatment of Ti metal." *J. Asian Ceram. Soc.*. vol. 9. no. 4. pp. 1448–1456. 2021. doi: 10.1080/21870764.2021.1979287.

[13] M. Honda. T. Ochiai. P. Listiani. Y. Yamaguchi. and Y. Ichikawa. "Nanostructures via Liquid Phase Deposition Method for." 2023.

[14] La Ode Asmin and L. Isa. "Synthesis and Characterization of Structural Nanocomposite Titanium Dioxide Copper-Doped Using the Impregnation Method." *Spektra J. Fis. dan Apl.*. vol. 5. no. 1. pp. 21–30. 2020. doi: 10.21009/spektra.051.03.

[15] L. Díaz *et al.*. "M/tio2(m = fe. co. ni. cu. zn) catalysts for photocatalytic hydrogen production under uv and visible light irradiation." *Inorg. Chem. Front.*. vol. 8. no. 14. pp. 3491–3500. 2021. doi: 10.1039/d0qi01311k.

[16] A. Adamu. M. Isaacs. K. Boodhoo. and F. R. Abegão. "Investigation of Cu/TiO2 synthesis methods and conditions for CO2 photocatalytic reduction via conversion of bicarbonate/carbonate to formate." *J. CO2 Util.*. vol. 70. no. October 2022. 2023. doi: 10.1016/j.jcou.2023.102428.

[17] D. KAYA and N. TÜRKTEN. "PREPARATION OF DOPED TiO2 PHOTOCATALYSTS AND THEIR DECOLORIZATION EFFICIENCIES UNDER SOLAR LIGHT." *Mühendislik Bilim. ve Tasarım Derg.*. vol. 8. no. 3. pp. 655–663. 2020. doi: 10.21923/jesd.672207.

[18] C. Y. Leong. H. L. Teh. M. C. Chen. and S. L. Lee. "Effect of Synthesis Methods on Properties of Copper Oxide Doped Titanium Dioxide Photocatalyst in Dye Photodegradation of Rhodamine B." *Sci. Technol. Indones.*. vol. 7. no. 1. pp. 91–97. 2022. doi: 10.26554/sti.2022.7.1.91-97.

[19] N. M. Deraz. "comparative jurisprudence of catalysts preparation methods: I. precipitation and impregnation methods.'. J. Ind. Environ. Chem.. vol. 2. no. 1. pp. 19–21. 2018.The comparative jurisprudence of catalysts preparation methods: I. precipitation and impregnati." *J. Ind. Environ. Chem.*. vol. 2. no. 1. pp. 19–21. 2018.

[20] A. Garg. A. Singh. V. K. Sangal. P. K. Bajpai. and N. Garg. "Synthesis. characterization and anticancer activities of metal ions Fe and Cu doped and co-doped TiO2." *New J. Chem.*. vol. 41. no. 18. pp. 9931–9937. 2017. doi: 10.1039/c7nj02098h.

[21] X. J. Yang. S. Wang. H. M. Sun. X. B. Wang. and J. S. Lian. "Preparation and photocatalytic performance of Cu-doped TiO2 nanoparticles." *Trans. Nonferrous Met. Soc. China (English Ed.*. vol. 25. no. 2. pp. 504–509. 2015. doi: 10.1016/S1003-6326(15)63631-7.

[22] V. Kavitha. P. S. Ramesh. and D. Geetha. "Synthesis of Cu loaded TiO2 nanoparticles for the improved photocatalytic degradation of Rhodamine B." *Int. J. Nanosci.*. vol. 15. no. 5–6. pp. 1–8. 2016. doi: 10.1142/S0219581X16600024.

[23] V. Krishnakumar. S. Boobas. J. Jayaprakash. M. Rajaboopathi. B. Han. and M. Louhi-Kultanen. "Effect of Cu doping on TiO2 nanoparticles and its photocatalytic activity under visible light." *J. Mater. Sci. Mater. Electron.*. vol. 27. no. 7. pp. 7438–7447. 2016. doi: 10.1007/s10854-016-4720-1.

[24] H. Abdelouahab Reddam. R. Elmail. S. C. Lloria. G. Monrós Tomás. Z. A. Reddam. and F. Coloma-Pascual. "Synthesis of Fe. Mn and Cu modified TiO2photocatalysts for photodegradation of Orange II." *Bol. la Soc. Esp. Ceram. y Vidr.*. vol. 59. no. 4. pp. 138–148. 2020. doi: 10.1016/j.bsecv.2019.09.005.

[25] C. Sahoo and A. K. Gupta. "Characterization and photocatalytic performance evaluation of various metal ion-doped microstructured TiO2 under UV and visible light." *J. Environ. Sci. Heal. - Part A Toxic/Hazardous Subst. Environ. Eng.*. vol. 50. no. 7. pp. 659–668. 2015. doi: 10.1080/10934529.2015.1011958.

[26] J. QADERI. C. R. MAMAT. and A. A. JALIL. "Preparation and Characterization of Copper . Iron . and Nickel Doped Titanium Dioxide Photocatalysts for Decolorization of Methylene Blue." *Sains Malaysiana*. vol. 50. no. 1. pp. 135–149. 2021. doi: 10.17576/jsm-2021-5001-14.

[27] E. L. Jacoski. "Sol-gel Synthesis and Spectroscopic Characterization of Titanium Dioxide Doped with Copper and Iron." 2022.

[28] M. Nafees. W. Liaqut. S. Ali. and M. A. Shafique. "Synthesis of ZnO/Al:ZnO nanomaterial: structural and band gap variation in ZnO nanomaterial by Al doping." *Appl. Nanosci.*. vol. 3. no. 1. pp. 49–55. 2013. doi: 10.1007/s13204-012-0067-y.

[29] M. Sahu and P. Biswas. "Single-step processing of copper-doped titania nanomaterials in a flame aerosol reactor." *Nanoscale Res. Lett.*. vol. 6. pp. 1–14. 2011. doi: 10.1186/1556-276X-6-441.

[30] G. Colón. M. Maicu. M. C. Hidalgo. and J. A. Navío. "Cu-doped TiO2 systems with improved photocatalytic activity." *Appl. Catal. B Environ.*. vol. 67. no. 1–2. pp. 41–51. 2006. doi: 10.1016/j.apcatb.2006.03.019.

[31] R. Ahmadiasl. G. Moussavi. S. Shekoohiyan. and F. Razavian. "Synthesis of Cu-Doped TiO2 Nanocatalyst for the Enhanced Photocatalytic Degradation and Mineralization of Gabapentin under UVA/LED Irradiation: Characterization and Photocatalytic Activity." *Catalysts*. vol. 12. no. 11. 2022. doi: 10.3390/catal12111310.

[32] M. K. Hossain. M. M. Hossain. and S. Akhtar. "Studies on Synthesis. Characterization. and Photocatalytic Activity of TiO2and Cr-Doped TiO2for the Degradation of p-Chlorophenol." *ACS Omega*. 2022. doi: 10.1021/acsomega.2c05107.

[33] A. B. Aritonang. A. Asma. and A. Sapar. "Synthesis of The Cu(II)-doped TiO2/Bi2O3 as a Photocatalyst for Rhodamin B Degradation Under Visible Light Ilumination." *Berk. Sainstek*. vol. 11. no. 4. p. 216. 2023. doi: 10.19184/bst.v11i4.39799.

[34] X. Dong *et al.*. "Bi-doped TiO2 with remarkably enhanced photocatalytic activity under simulated sunlight induced by increased hydrophilicity and light absorption ability." *J. Adv. Oxid. Technol.*. vol. 17. no. 1. pp. 39–43. 2014. doi: 10.1515/jaots-2014-0105.

[35] E. H. A. N. Ma'rifah. A. Supriyanto. T. Paramitha. H. Widiyandari. A. Purwanto. and H. K. K. Aliwarga. "Titanium Dioxide (TiO2) Doping Copper (Cu) with Annealing Temperature Variation as Photoanode for Dye-Sensitized Solar Cells (DSSC)." *E3S Web Conf.*. vol. 465. 2023. doi: 10.1051/e3sconf/202346502065.

[36] H. Yan. T. Zhao. X. Li. and C. Hun. "Synthesis of Cu-doped nano-TiO2 by detonation method." *Ceram. Int.*. vol. 41. no. 10. pp. 14204–14211. 2015. doi: 10.1016/j.ceramint.2015.07.046.